TECHNICAL ARTICLE

Ion size effect on chemical bonds of the RBa$_2$Cu$_{2.9}$Zn$_{0.1}$O$_y$ system

R. Benredouane,[1,2,a)] and C. Boudaren[1]

[1]*Unité de Recherche de Chimie de l'Environnement et Moléculaire Structurale, CHEMS, Département de Chimie, Université Frères Mentouri Constantine, Constantine 25000, Algeria*

[2]*Département de Physique et Chimie, Ecole Normale Supérieure d'Enseignements Techniques (ENSET), Skikda 21000, Algeria*

Single-phase polycrystalline samples of RBa$_2$Cu$_{2.9}$Zn$_{0.1}$O$_y$ (R = Y, Nd, Gd, Er, and Tm) (ZnR123) were synthesized using the standard solid-state reaction method. They were characterized by X-ray powder diffraction (XRD) and scanning electron microscope. XRD shows that all samples consist essentially of a single phase and retain the orthorhombic structure. The structure of the samples was refined by the Rietveld method with the help of the bond valence sum method. The variation of the lattice parameters and some meaningful bond angles and lengths with the ionic radius are discussed. In these compounds, the variations of the buckling angles Cu2–O(2,3)–Cu2 and Cu2–Cu2–O(2,3) are unique: the bond angles Cu–O3–Cu2 and Cu2–Cu2–O2 increase, whereas the bond angles Cu2–O2–Cu2 and Cu2–Cu2–O3 decrease. The variation of these bond angles brings about a strong curvature of the Cu2O plane. Furthermore, we have found tree fixed triangles formed by the Cu2, O2, and O3 atoms in addition to another fixed triangle O1–Ba–O1 observed for the first time. BVS of Cu2 atom shows a specific and unique variation compared with other compounds. © *2018 International Centre for Diffraction Data.* [doi:10.1017/S0885715618000520]

I. INTRODUCTION

Cuprate perovskite compounds with the general formula RBa$_2$Cu$_3$O$_{7-\delta}$ (R123) (R = rare-earth elements and Y) have a layered structure, which consists of alternating blocks with perovskite and rock-salt arrangements. These compounds are superconductors (notable exceptions are Ce, Pr, and Tb). The critical temperature T_c increases monotonically with increasing ionic radius from 88 to 94 K (Lin *et al*., 1995; Williams and Tallon, 1996; Chen *et al*., 2006). The Cu2O layers responsible for superconductivity are located in the perovskite block. The rock-salt blocks provide the stability of the structure and play the role of charge reservoir, as they create the necessary hole concentration in the conducting band for the appearance of superconductivity. These compounds attracted a great deal of interest. A lot of efforts have been devoted to the study of how different types of substitutions would influence their structural and superconductive properties.

The substitution of Zn atoms at Cu sites in R123 requires more attention. It mainly substitutes the plane Cu2 sites and causes keen depression of superconductivity, even though it is a non-magnetic ion (Xu *et al*., 1996).

The reduction of T_c for RBa$_2$Cu$_{3-x}$Zn$_x$O$_{7-\delta}$ is found to depend strongly on the ionic radius of the rare-earth element R. A strong suppression in T_c at the rate of 28 K/at.% in the system NdBa$_2$(Cu$_{1-y}$Zn$_y$)$_3$O$_{7-\delta}$ is reported (Marv *et al*., 1993; Jamadar *et al*., 2013). This effect resembles the ion size effect on T_c in R_{1-x}Pr$_x$Ba$_2$Cu$_3$O$_{7-\delta}$, where Pr substitutes on the R site, in RBa$_2$Cu$_{3-x}$Ga$_x$O$_{7-\delta}$, where Ga substitutes on the Cu1 sites in Cu1O chains, and in RBaSrCu$_3$O$_y$ (Awana *et al*., 2000a).

It is noticeable that a few detailed works about the structural properties of the compounds RBa$_2$Cu$_{2.9}$Zn$_{0.1}$O$_{7-\delta}$ are reported within our knowledge: Zn-Y123 (Kajitani *et al*., 1988; Xiao *et al*., 1988; Maeda *et al*., 1989; Mazumder *et al*., 1989; Balagurov *et al*., 1996) and Zn-Er123 (Podlesnyak *et al*., 1991). Our research paper will shed light on the subtle structural changes of the RBa$_2$Cu$_{2.9}$Zn$_{0.1}$O$_y$ system (ZnR123) (R = Nd, Gd, Y, Er, and Tm). The central aim of the present work is to investigate the effect of the R ions size on the structure of the system RBa$_2$Cu$_{2.9}$Zn$_{0.1}$O$_y$ toward a better understanding of the relationship between the structure and the superconductivity in these materials. Rietveld refinements of X-ray powder diffraction (XRD) data for ZnR123 samples are used to determine our structural parameters. These parameters will be used for the bond-valence sum (BVS) calculations.

II. EXPERIMENTAL

A. Synthesis of powders

Polycrystalline samples of RBa$_2$Cu$_{2.9}$Zn$_{0.1}$O$_y$ (R = Nd, Gd, Y, Er, Tm) were prepared via a solid-state reaction technique. The raw materials of R_2O$_3$, BaCO$_3$, CuO, and ZnO were thoroughly mixed in the proper ratio and calcined at 900 °C for 48 h in an air atmosphere and then quenched them to room temperature. Calcination was repeated with intermediate grinding until X-ray-diffraction (XRD) analysis

confirmed the formation of a single-phase compounds. All samples were prepared under identical conditions.

B. Characterization

The XRD measurements have been done by Bruker D5000 powder diffractometer provided with a graphite monochromator and using CuKα radiation. The radiation was detected by a scintillation counter. The other measured parameters were a tube voltage of 40 kV and a tube current of 30 mA, goniometer radius of 125 mm, slit sizes: aperture 1 mm, scattered radiation 2 mm, and detector 0.6 mm. Patterns were measured at room temperature from 20° to 120° 2θ in 0.02° step width, counting for 10 s step.

Structure refinements were performed with the Rietveld method (Rietveld, 1969) using the FULLPROF software (Rodríguez-Carvajal, 1990) and the orthorhombic space group *Pmmm*. The wavelengths of CuKα₁, CuKα₂, and the intensity ratio were 1.540560 Å, 1.544330 Å, and 0.514, respectively. For structure refinement, most atomic positions were considered to be fully occupied, with the exception of the chain oxygen O4, and the O5 position along the *a*-axis direction, in order to register any oxygen disorder. The isotropic thermal displacements (Biso) of the oxygen atoms were fixed to 0.4 Å². Cava *et al.* (1990) reported that the Biso of oxygen atoms in the orthorhombic Y123 compound changes between 0.15 and 0.71 Å². So, we choose the mean value of this range.

The scanning electron microscopy (SEM) measurements have been done to determine the grain size and homogeneity of the samples by the JEOL JSM-5900 instrument. No impurities were observed.

C. BVS calculations

Analysis of BVS has emerged as a simple but powerful tool to investigate the structures and superconducting properties of cuprates (Cava *et al.*, 1990; Brown, 1991; Tallon, 1991; Williams and Tallon, 1996). BVS calculation were performed using a method similar to that described in detail previously (Lundqvist *et al.*, 1996). Therefore, only a few details are mentioned below. The atomic valence of an atom is assumed to be distributed between the bonds that it forms. BVS of atom *i*, denoted V_i, is then $V_i = \sum_j S_j = \sum \exp[(R_0 - R_{ij})/0.37]$, where S_j is the valence of one bond, and the sum is over all neighbors *j* (Brown and Shannon, 1973). The constant 0.37 was empirically determined (Brown and Altermatt, 1985). R_0 represents the length of a bond of a unit valence (Brown and Altermatt, 1985), and R_{ij} is the experimentally determined distance between atoms *i* and *j*. The BVS were calculated using the formulas suggested by Brown and Altermatt (Brown and Altermatt, 1985) and implemented in FULLPROF.

BVS for oxygen was obtained by taking into account the valence of Cu (Lundqvist *et al.*, 1996). The BVS of the plane copper is $S(Cu2) = S(Cu2)n_{Cu2} + S(Zn)n_{Zn}$, where n_{Cu2} and n_{Zn} are the occupancies of Cu and Zn at the copper site Cu2, respectively.

The distribution of charge in Cu2O planes can be characterized by the advanced BVS model of Tallon (1991; Williams and Tallon, 1996). In this model, the hole concentration on the Cu2O planes is described by the parameter $V_- = 2 + V_{Cu2} - V_{O2} - V_{O3}$ where V_{Cu2}, V_{O2} and V_{O3} are the values of BVSs about the planer Cu2, O2 and O3 atoms, respectively. Another parameter, namely, $V_+ = 6 - V_{Cu2} - V_{O2} - V_{O3}$, is a measure of both lattice stress and charge distribution between Cu and O atoms.

III. RESULTS AND DISCUSSION

A. SEM results

The SEM topographs of the samples show a homogeneous stone-like grains with a typical size of several microns (Figure 1). This picture depicts that the average grain size decreases with the decrease of the ionic radius.

B. Rietveld refinement

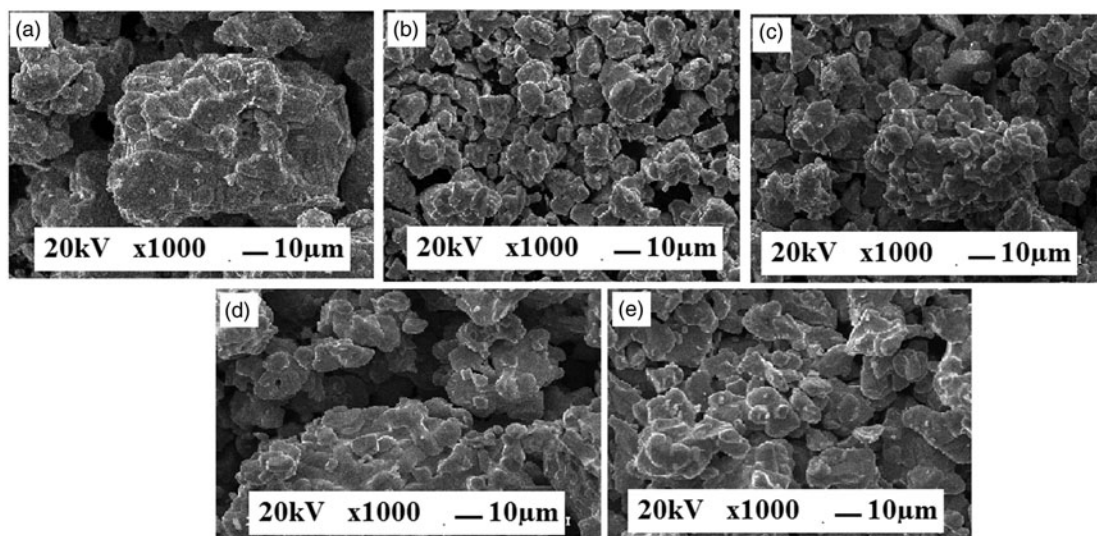Figure 2 displays the XRD profiles of ZnR123 at room temperature. These patterns indicate that the compounds of

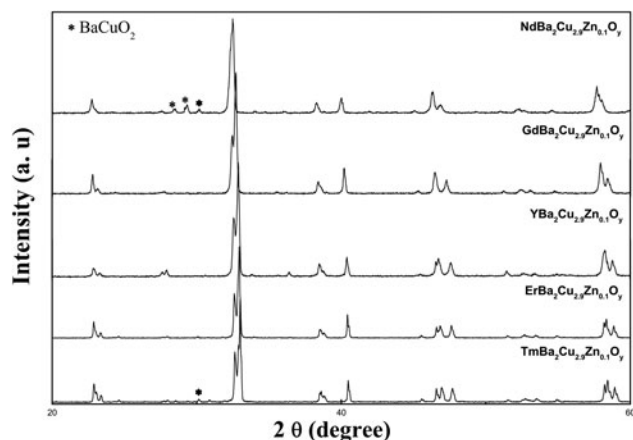Figure 1. SEM micrographs of our samples (a) ZnNd123, (b) ZnGd123, (c)ZnY123, (d) ZnEr123, and (e) ZnTm123.

Figure 2. X-ray powder diffraction patterns for samples.
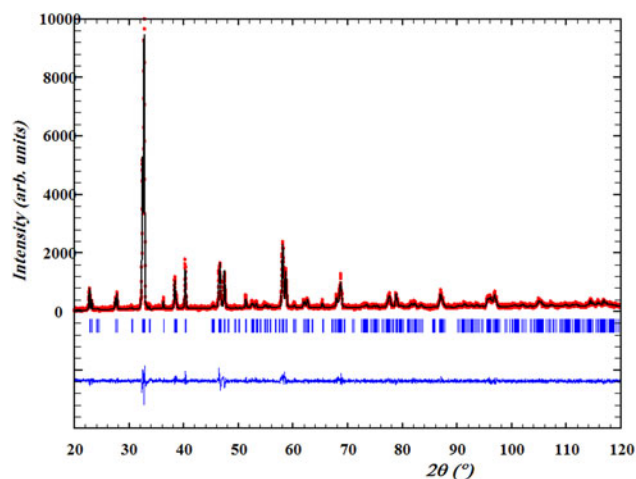

Figure 3. (Color online) Rietveld refinement profiles of YBa$_2$Cu$_{2.9}$Zn$_{0.1}$O$_y$. The black line is the measurement results and the red line is the calculated profile. The vertical short line represents the position of the Bragg reflections. The difference curves were plotted at the bottom.

nominal composition with R = Nd, Gd, Y, Er, and Tm have a single-phase orthorhombic perovskite-like YBa$_2$Cu$_3$O$_{7-\delta}$ structure. For samples ZnNd123 and ZnTm123, there are secondary phases belonging to BaCuO$_2$ (noted as 011) phase.

The reflections of this phase were excluded from the refinements.

A typical Rietveld refinement profile is presented in Figure 3; the results show that the structure remains orthorhombic with the space group *Pmmm*. We do not discuss here the oxygen occupancy because of the weak X-ray scattering power of the oxygen atoms. But, according to the study of Liyanawaduge *et al.* (2010), we can say that our samples annealed in air are oxygen-deficient. Furthermore, the oxygen content is constant for the current series because of their synthesis under the same conditions. According to the refined *R*-factors and the difference curves (the experimental curve minus the fitted one), we believe that these refinements are good.

The lattice parameters for the RBa$_2$Cu$_{2.9}$Zn$_{0.1}$O$_y$ series of samples, where R = Y, Nd, Gd, Er, and Tm, were determined by Rietveld refinements. The lattice constants and unit-cell volumes vs. ionic radius are depicted in Figure 4(a). The lattice constants of the compounds ZY123 and ZEr123 are comparable with the lattice constants of other ZY123 and ZEr123 compounds (PDF 01-080-0855, Mazumder *et al.*, 1989, PDF 01-086-0023, Podlesnyak *et al.*, 1991). It may be noticed that the lattice parameters, as well as the volume of the unit cell, increase as the ionic radius increases. This increase can be related to the size effect because of the variation in atomic volume, which results from R replacing for Y.

The relative changes of the lattice constants of a and b can be recognized from the normalized orthorhombic strain, which was calculated from the formula $\eta = 2(b - a)/(b + a)$.

The orthorhombic strain is plotted in Figure 4(b). We can see that it increases and then decreases as the ionic radius increases. This is in contrast to the observation in fully oxygenated R123 (Guillaume *et al.*, 1994) where it decreases as the ionic radius increases.

C. Bond lengths and angles

The bond lengths and angles are derived from the refined results. For a convenient discussion, the crystalline structure is illustrated in Figure 5, the positions of atoms and some chemical bonds are indicated.

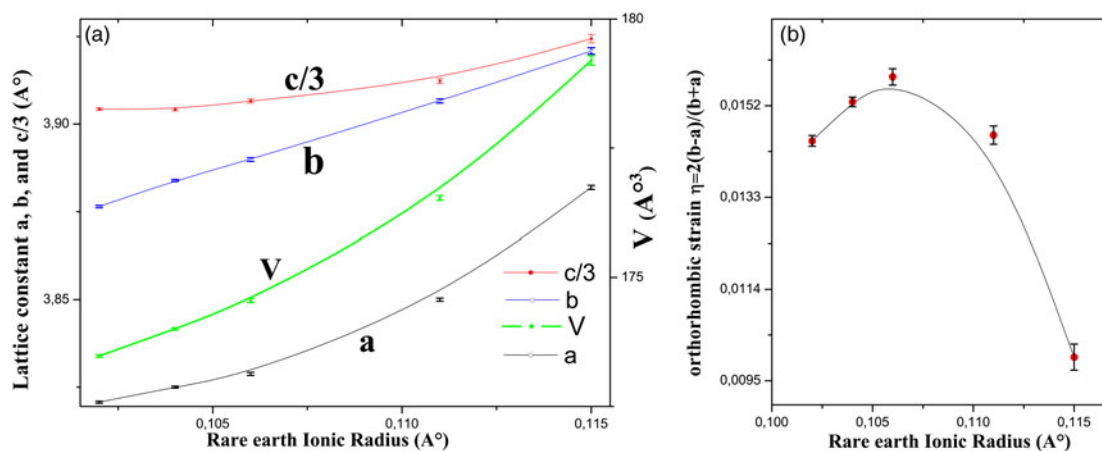The bond angles Cu2–O2–Cu2, Cu2–O3–Cu2, Cu2–Cu2–O2, and Cu2–Cu2–O3 are called buckling angles.

Figure 4. (Color online) (a) Lattice constants and the unit-cell volume. (b) Orthorhombic strain. Error bars are equal to three estimated standard deviation (ESD) obtained from the Rietveld refinement.
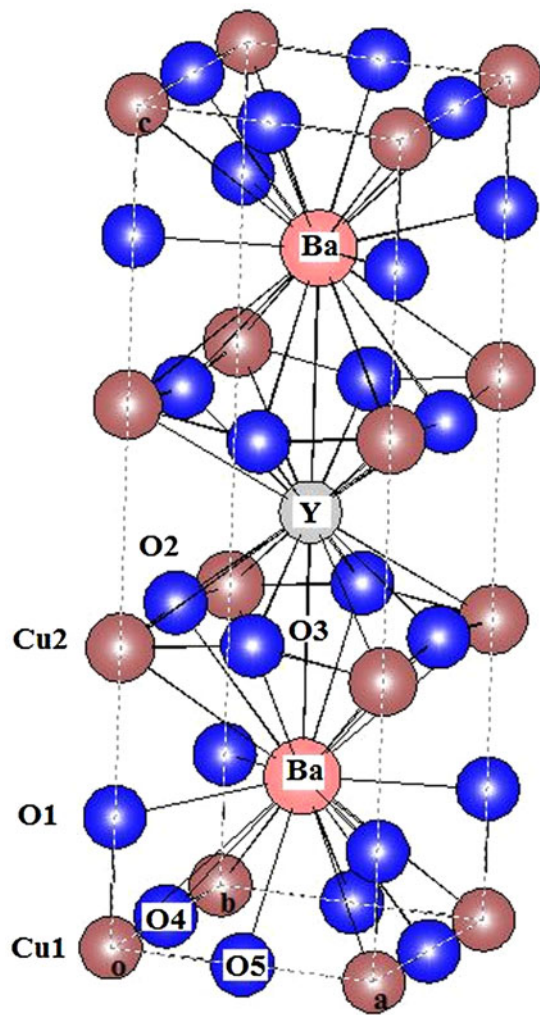
Figure 5. (Color online) Crystalline structure of Zn*R*Cu1212, in which the bonds are indicated.

These bond angles affect directly the curvature of the Cu2O plane.

The bond angles Cu2–Cu2–O2 and Cu2–O3–Cu2 increase at the same time that Cu2–Cu2–O3 and Cu2–O2–

Cu2 decrease, with increasing ionic radius and lowering T_c [Figures 6(a) and 6(b)]. It is worth mentioning that these variations bring about a strong curvature of the Cu2O plane.

The bond angle Cu2–O2–Cu2 increases with lowering T_c in the compounds $NdBa_{2-x}Nd_xCu_3O_y$ and $NdBa_{2-x}Pr_xCu_3O_y$ (Kramer *et al.*, 1997), and in the compound $Er_{1-x}Ca_xBa_2 Cu_3O_y$ (Awana *et al.*, 2000b). This bond angle also increases with lowering T_c in the self-compensating Y(Ca)Ba(La)123 system accompanied with the decrease of the bond angle Cu2–O3–Cu2 (Jin *et al.*, 2010).

In the system $Nd_{1-x}Pr_xBa_2Cu_3O_y$, the bond angles Cu2–Cu2–O(2,3) increase simultaneously with the decrease of T_c (Ghorbani *et al.*, 2004).

This strong curvature of the Cu2O plane found in our compounds is also confirmed by the decrease of the bond angle O3–*R*–O3 and the increase of the bond angle O3–Ba–O3 with the augment of ionic radius and the descent of T_c (Figure 7).

These results indicate that the O3 atom has some displacement along the *c*-axis; approaching the BaO layer and away from the *R* atom layer. This displacement of the O3 atom is in contradiction to its displacement in the self-compensating Y(Ca)Ba(La)123 system with lowering T_c (Jin *et al.*, 2010).

We find that the angles O2–Cu2–O2, O3–Cu2–O3, and O2–Cu2–O3 are very stable (changing range from 62.72 to 63.66° for the two first ones and 87.94– 89.8° for the last one). Yu *et al.* also found a stable angle O2–Cu2–O3 changes between 88.7 and 89.5° in the Y(Pr)123 system and they called it "fixed triangle", which is independent of the doping level in their system (Yu *et al.*, 2009). They concluded that their fixed triangle is located in between the perovskite block and the rock-salt block (Jin *et al.*, 2009). In the Y(Pr) 123 system, the distances Cu2–O2 and Cu2–O3 are also fixed (Yu *et al.*, 2009).

According to Figure 8, the bond angle O1–Ba–O1 that is situated in the BaO layer form a stable triangle. This bond angle is also situated between the perovskite block and the rock-salt block. Within our knowledge, this result has never been cited.

We can also notice the decrease of the bond angle O3–Cu2–O1 (Figure 8) which is in contradiction with its increase in the self-compensating Y(Ca)Ba(La)123 system, with the
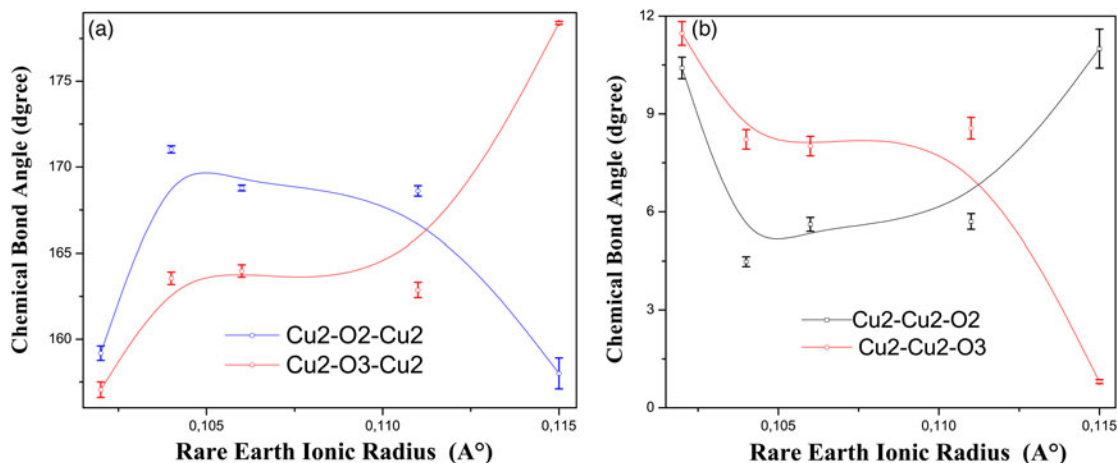

Figure 6. (Color online) The variation of the buckling angles with the ionic radius of Y and rare-earth elements. Error bars are equal to three estimated standard deviation (ESD) obtained from the bond angles calculations.
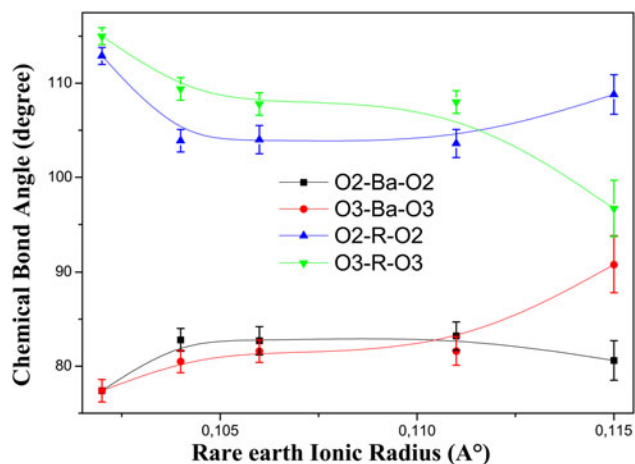
Figure 7. (Color online) The variation of bond angles between central atoms R and Ba and the Cu2O plane. Error bars are equal to three estimated standard deviation (ESD) obtained from the bond angles calculations.

Figure 9. (Color online) Bond lengths of Cu2, Cu1, Ba, and O1 atoms. Error bars are equal to three estimated standard deviation (ESD) obtained from the bond lengths calculations.

descent of T_c, which contributes to the curvature of the Cu2O plane (Jin *et al.*, 2010). So, the decrease of the bond angle O3–Cu2–O1 in our compounds confirm our preceding results about the displacement of the O3 atom toward the BaO layer.

Figure 9 shows bond lengths formed by the Cu2, Cu1, and Ba atoms. The distance Cu1–O1 decreases then increases slightly by about 0.04A°. This distance varies in the same way as the orthorhombic strain but in the opposite direction. On the other hand, the bond length Cu2–O1 decreases markedly with increasing ionic radius and lowering T_c. The decrease of this latter is also reported in the system Y(Pr) 123 with lowering T_c (Yu *et al.*, 2009). In the pure Y123 and Er123 compounds, the distance Cu2–O1 increases markedly at the same time that the distance Cu1–O1 decreases slightly, with oxygen removal and the lowering of T_c (Rupp *et al.*, 1989; Cava *et al.*, 1990). In the system $Nd_{1-x}Pr_xBa_2Cu_3O_y$ with $x < 0.2$, the distance Cu1–O1 is constant but the distance Cu2–O1 shows a slight decrease (Ghorbani *et al.*, 2004).

So, we can conclude that there is a positive correlation between T_c and the Cu2–O1 bond length. The Cu2–O1 bond is just located between the perovskite block and the rock-salt block and connects them (Zhang *et al.*, 2000). Jin *et al.* said that the weakening of the interaction between the two structural blocks corresponds to the lengthening of this chemical bond and then the increase of T_c in the self-compensating Y(Ca)Ba(La)123 system from the underdoped region to the overdoped region (Jin *et al.*, 2009). This is exactly the situation in our compounds.

The Ba site is located between the Cu2O superconducting plane and the Cu1O charge reservoir chains (Jorgensen *et al.*, 1990), which both have proved to be essential for superconductivity of 123 systems. We remark that the Ba atoms become closer to the plane Cu2O and farther from the Cu1O chain by the slight decrease of the distance Ba–Cu2 and the slight increase of the distance Ba–Cu1 (Figure 9). The Ba displacement toward the Cu2O plane is very clear for $R = Nd$. In addition to that, the distance Ba–O1 increases slightly with increasing ionic radius and lowering T_c (Figure 9). This slight increase is also found in the pure Y123 compound with oxygen removal (Cava *et al.*, 1990) and in the Y(Pr)123 system with increasing Pr content (Kinoshita *et al.*, 1988). We can directly relate this increase to the increase of the c-lattice parameter, but it is important in preventing the charge transfer from Cu1O chains to Cu2O planes, which takes place through the O(1) atom. We can also notice the stability of Ba–O4 distance and its noticeable increase for $R = Nd$ (Figure 9). Cava *et al.* (1990) reported the slight increase of this distance in the pure Y123 compound with oxygen removal and lowering T_c.

D. Bond-valence sum

In order to estimate the effect of varying bond distances on the valences of different atoms, it is useful to calculate BVS. Although, this method is empirical, it can nevertheless help to identify important trends when a series of related and similarly prepared samples are compared. Our results for the BVS are shown in Figure 10 for the present $RBa_2Cu_{2.9}Zn_{0.1}O_y$ samples.

The various strains encountered in the R123 system can be better understood in terms of the bond valences at the rare-earth and barium ions. The valence sums calculated around R and Ba atoms are shown in Figure 10(a). Except for Tm, the bond valences on the rare earths show a smooth
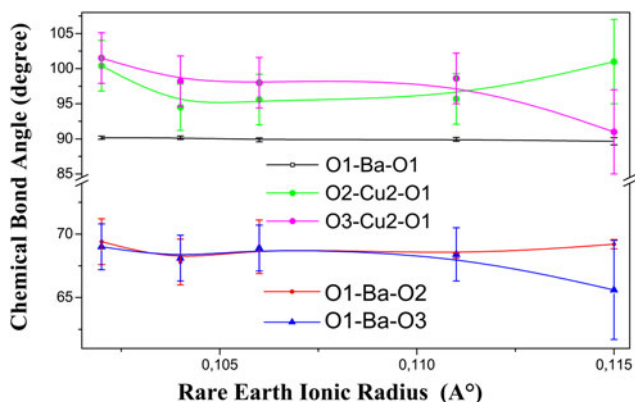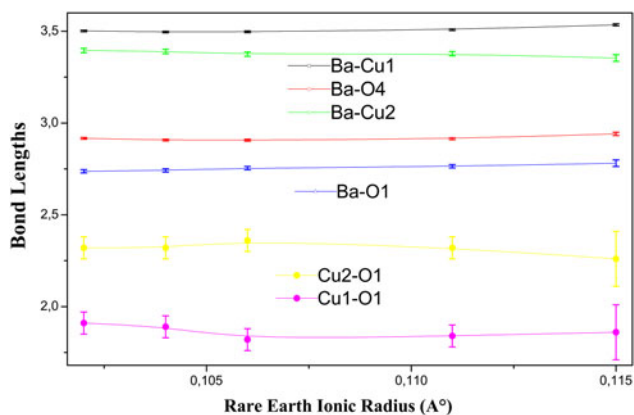

Figure 8. (Color online) The variation of some bond angles located in the BaO and between it and the Cu2O plane with the ionic radius of Y and rare-earth elements content. Error bars are equal to three estimated standard deviation (ESD) obtained from the bond angles calculations.
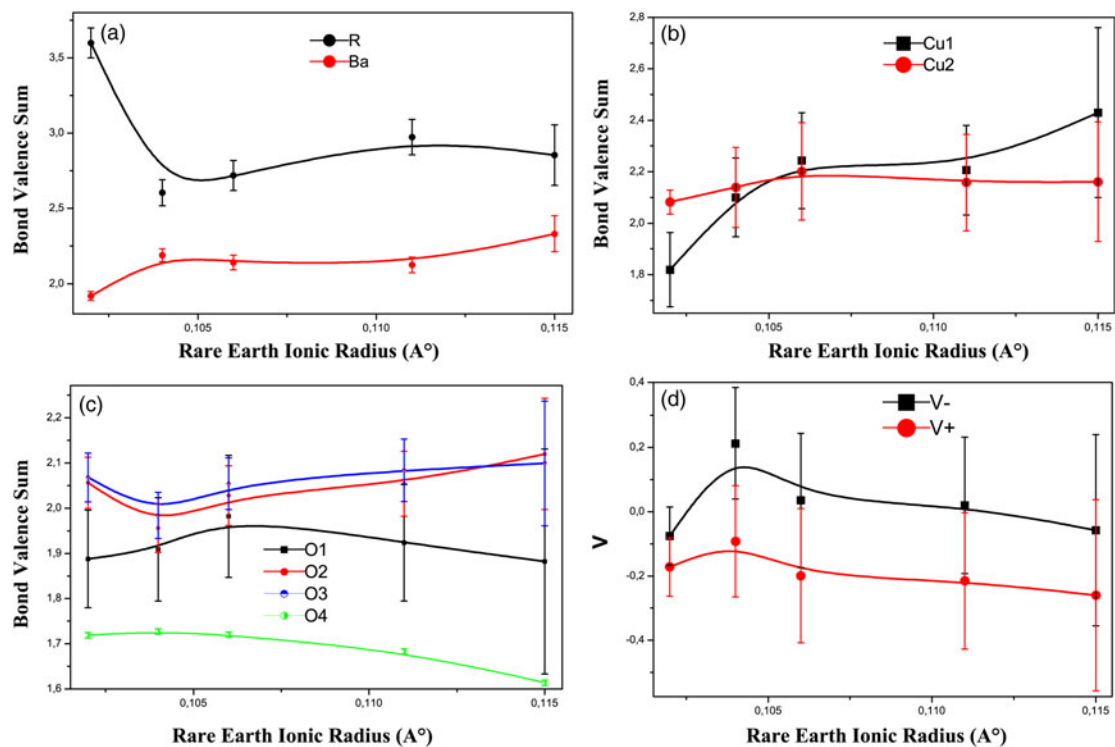
Figure 10. (Color online) The BVS of atoms in the $RBa_2Cu_{2.9}Zn_{0.1}O_y$ system vs. rare earths ionic radius. (a) For Ba and R. (b) For Cu1 and Cu2. (c) For O1, O2, O3, and O4. (c) V_- and V_+. Error bars are equal to three estimated standard deviation (ESD) obtained from the BVS calculations.

increase with increasing ionic radius like the pure compound (Ramesh and Hegde, 1994). We can observe that the R BVS is between 2.604 and 2.973, which represents a reasonable agreement with +3. The BVS value calculated for Tm is 3.599, and there is a considerable deviation from the expected value of the corresponding ion. This indicates that the Tm sublattice is highly strained and it needs a correction through a specific method mentioned in Pinto's article (Pinto *et al.*, 1997).

The BVS of the Ba atom increases with increasing ionic radius and varies between 1.919 and 2.332 [Figure 10(a)]. Therefore, there is a change in geometric stress (the coordination polyhedron is too small for Ba with the large ion Nd and with the small ion Tm).

The BVS of the Cu1 atom increases with lowering T_c, which is in good agreement with the pure R123 compounds (Samoylenkov *et al.*, 1997). On the other hand, the Cu2 atom BVS increases then decreases. In the pure R123, the bond valences at the Cu2 site increase with decreasing rare-earth radius and lowering T_c (Ramesh and Hegde, 1994; Samoylenkov *et al.*, 1997).

Figure 10(c) shows the variation of BVS of oxygen atoms. The bond valences on the oxygen atoms O(2), O(3) in addition to the apical oxygen O(1) did not show a marked deviation from the ideal valency. However, the oxygen ions at O(4) site show a significant lower value of bond valence from the nominal value, suggesting that this oxygen site is more likely to share the holes on copper to a certain extent.

The decrease of Cu2 BVS signifies the decrease of the hole concentration on Cu2O planes. We can confirm this result by the calculation of the V_- parameter. The total hole doping in the plane V_- decreases with increasing ionic radius and lowering T_c [Figure 10(d)]. This decrease of the V_-

parameter with lowering T_c is also shown in the system $Nd_{1-x}Pr_xBa_2Cu_3O_{7-\delta}$ (Ghorbani *et al.*, 2004). The total hole density in the planes was suggested by Tallon (Tallon, 1990) to correlate with the variation of T_c between alloys with varying charge. The preference for holes to go to the oxygen atoms in the Cu2O plane, V_+, was linearly correlated by Tallon to the maximum attainable T_c in a particular alloy system. In our case, V_+ decreases with increasing ionic radius and lowering T_c [Figure 10(d)], which is in good agreement with the $Nd_{1-x}Pr_xBa_2Cu_3O_{7-\delta}$ system (Ghorbani *et al.*, 2004).

IV. CONCLUSION

The results of the microstructural study of $RBa_2Cu_{2.9}Zn_{0.1}$ system with R = Y, Nd, Gd, Er, and Tm shows that the average grain size is found to decrease with decreasing the ionic radius.

Through a detailed structural of the above mentioned compounds, we have found that the buckling angles Cu2–Cu2–O2 and Cu2–O3–Cu2 increase at the same time when Cu2–Cu2–O3 and Cu2–O2–Cu2 decrease. In addition to that, the bond angles O3–R–O3 and O3–Cu2–O1 decrease simultaneously as O3–Ba–O3 increases.

The variation of these bond angles brings about a strong curvature of the Cu2O plane. The nature of this curvature is noticeably different from the ones found in any other compound. As a matter of fact, it is widely recognized that there is a good correlation between the curvature of the Cu2O plane and the apparition of superconductivity.

We have also noticed the existence of three fixed triangles formed by the Cu2, O2, O3 atoms in addition to another fixed triangle O1–Ba–O1 observed for the first time. We can notice here that these fixed triangles are situated in the boundary of

the perovskite block and the rock-salt block. We have also found a decrease in the apical distance Cu2–O1 with increasing ionic radius and lowering T_c. In addition to that, BVS of Cu2 increases then decreases. Its variation is unique compared with its variation in other compounds cited in previous research papers.

SUPPLEMENTARY MATERIAL

ACKNOWLEDGEMENT

Awana, V. P. S., Malik, S. K., Cardoso, C. A., De Lima, O. F., Cupta, A., Sedky, A., Yelon, W. B., Prasad, R. and Narlikar, A. V. (**2000a**). "Strong dependence of superconducting transition temperature (Tc) on the rare earth ionic size in REBaSrCu₃O₇ (RE = Y, Dy, Nd and La) series", Mod. Phys. Lett. B **12**, 361–372.

Awana, V. P. S., Malik, S. K., Yelon, W. B., Cardoso, C. A., de Lima, O. F., Anurag, G., Sedky, A., and Narlikar, A. V. (**2000b**). "Neutron diffraction on $Er_{1-x}Ca_xBa_2Cu_3\text{-}O_{7-\delta}$ ($0.0 \leqslant x \leqslant 0.3$) system: possible oxygen vacancies in CuO₂ planes", Phys. C **338**, 197–204.

Balagurov, A. M., Sikolenko, V. V., Simkin, V. G., Parfionov, O. E., and Shilshtein, S. Sh. (**1996**), "Neutron-diffraction study of $YBa_2Cu_{2.7}Zn_{0.3}O_{6+y}$ isotope enriched samples", Phys. C **259**, 173–180.

Brown, I. D. (**1991**). "The influence of internal strain on the charge distribution and superconducting transition temperature in Ba₂YCu₃O$_x$", J. Solid State Chem. **9**, 155–167.

Brown, I. D. and Altermatt, D. (**1985**). "Bond-valence parameters obtained from a systematic analysis of the inorganic crystal structure database", Acta Crystallogr. B **41**, 244–247.

Brown, I. D. and Shannon, R. D. (**1973**). "Empirical bond-strength-bond-length curves for oxides", Acta Crystallogr. **A29**, 266–282.

Cava, R. J., Hewat, A. W., Hewat, E. A., Batlogg, B., Marezio, M., Pabe, K. M., Drajewski, J. J., Peck, W. F. Jr., and Rapp, L. W. Jr. (**1990**). "Structural anomalies, oxygen ordering and superconductivity in oxygen deficient Ba₂YCu₃O$_x$", Phys. C **165**, 419–433.

Chen, Z., Zhang, J., Su, Y., Xue, Y., and Cao, S. (**2006**). "Effect of rare-earth ion size on local electron structure in RBa₂Cu₃O$_{7-\delta}$ (r = Tm, Dy, Gd, Eu, Nd and Y) superconductors: a positron study", Phys. C **434**, 161–166.

Ghorbani, S. R., Andersson, M., and Rapp, Ö. (**2004**). "Neutron diffraction studies of $Nd_{1-x}Pr_xBa_2Cu_3O_{7-\delta}$: evidence for hole localization", Phys. Rev. B **69**, 014503–014513.

Guillaume, M., Allenspach, P., Henggeler, W., Mesot, J., Roessli, B., Staub, U., Fischer, P., Furrer, A., and Trounov, V. (**1994**). "A systematic low-temperature neutron diffraction study of the RBa₂Cu₃O$_x$ (R = yttrium and rare earths; x = 6 and 7) compounds", J. Phys. Condens. Matter **6**, 7963–7976.

Jamadar, T. A., Roy, A., and Gosh, A. K. (**2013**). "Suppression of critical temperature and charge localization in underdoped NdBa2Cu3-xZnxO7-y", Phys. C **492**, 59–63.

Jin, W., Hao, S., and Zhang, H. (**2009**). "The fixed triangle chemical bond and its effect in the Y1-xCaxBa2-yLayCu3OZ system from underdoped to overdoped", New J. Phys. **11**, 113036–113051.

Jin, W. T., Hao, S. J., Zhang, X. J., Zhao, Y., and Zhang, H. (**2010**). "Bond angle study of self-compensating Y$_{1-x}$Ca$_x$Ba$_{2-x}$La$_x$Cu₃O$_z$ system", J. Supercond. Nov. Magn. **23**, 847–850.

Jorgensen, J. D., Veal, B. W., Paulikis, A. P., Nowicki, L. J., Grabtree, G. W., and Kwok, W. K. (**1990**). "Structural properties of oxygen-deficient YBa2Cu3O7-δ", Phys. Rev. **B41**, 1863–1877.

Kajitani, T., Kusaba, K., Kikuchi, M., Syono, Y., and Hirabayashi, M. (**1988**). "Crystal structures of $YBa_2Cu_{3-\delta}A_\delta O_{9-\gamma}$ (a = Ni, Zn and Co)", Jpn. J. Appl. Phys. **27**, L345–L357.

Kinoshita, K., Matsuda, A., Shibata, H., Ishii, T., Watanabe, T., and Yamada, T. (**1988**). "Crystal structure and superconductivity in $Ba_2Y_{1-x}Pr_xCu_3O_{7-y}$", Jpn. J. Appl. Phys. **27**, L1642–L1645.

Kramer, Y. M. J., Dennis, K. W., Falzgraf, D., and McCallum, R. W. (**1997**). "Suppression of superconductivity in the $R(Ba_{1-z}R_z)_2Cu_3O_{7+\delta}$ (r = Pr, Nd) system", Phys. Rev. B **56**, 5512–5517.

Lin, J. G., Huang, C. Y., Xue, Y. Y., Chu, C. W., Cao, X. W., and Ho, J. C. (**1995**). "Origin of the R-ion effect on Tc in RBa₂Cu₃O₇", Phys. Rev. B **51**, 12900–12903.

Liyanawaduge, N. P., Singh, S. K., Kumar, A., Awana, V. P. S., and Kishan, H.(**2010**). "Superconducting and magnetic properties of Zn-doped YBa2Cu3O7-δ", J. Supercond. Nov. Magn. **24**, 1599–1605.

Lundqvist, P., Tengroth, C., Rapp, O., Tellgren, R., and Hegedüs, Z. (**1996**). "Neutron-diffraction studies and interatomic distances in Ca-Pr doped $NdBa_2Cu_3O_{7-\delta}$", Phys. C **269**, 231–241.

Maeda, H., Koizumi, A., Bamba, N., Takayama-Muromachi, E., Izumi, F., Asano, H., Shimizu, K., Moriwaki, H., Kuroda, Y., and Yamazaki, H. (**1989**). "EXAFS and neutron diffraction studies of local and average structures for $YBa_2Cu_{2.8}Zn_{0.2}O_{7-\delta}$", Phys. C **157**, 483–490.

Marv, T. A., Kumar, N. R. S., and Varadaraju, U. V. (**1993**). "Influence of Cu-site substitution on the structure and superconducting properties of the $NdBa_2Cu_{3-x}M_xO_{7+\delta}$ (m = Fe, Co) and $NdBa_2Cu_{3-x}M_xO_{7+\delta}$ (m = Ni, Zn) systems", Phys. Rev. B **48**, 16727–16736.

Mazumder, S., Rajagopal, H., Sequeira, A., Singh, J., Rajarajan, A. K., Gupta, L. C., and Vijayaraghavan, R. (**1989**). "Structural and superconducting behaviour of Mg- and Zn-substituted YBa₂Cu₃O$_{7-\delta}$", Phase Transit. **19**, 97–105.

Pinto, R., Gupta, L. C., Sharma, R., Sequiera, A., and Gnanasekar, K. I. (**1997**). "Superconductivity in Lu$_{1-x}$Ca$_x$Ba₂Cu₃O$_{6+\delta}$", Phys. C **289**, 280–290.

Podlesnyak, A., Kozhevnikov, V., Mirmelstein, A., Allenspach, P., Mesot, J., Staub, U., Furrer, A., Osborn, R., Bennington, S. M., and Taylor, A. D. (**1991**). "Neutron spectroscopic studies of crystalline electric fields in high-Tc ErBa2Cu3O7 doped with Zn and Ni", Phys. C **175**, 587–594.

Ramesh, S. and Hegde, M. S. (**1994**). "Bond-valence analysis of the charge distribution and internal stresses in the RBa₂Cu₃O$_{7-\delta}$", Phys. C **230**, 135–140.

Rietveld, H. M. (**1969**). "A profile refinement method for nuclear and magnetic structures", J. Appl. Crystallogr. **2**, 65–71.

Rodríguez-carvajal, J. (**1990**). "FULLPROF: A program for Rietveld refinement and pattern matching analysis," Satellite Meeting on Powder Diffraction of the XV Congress of the IUCr, Toulouse, France, P. 127.

Rupp, B., Pörschke, E., Meuffels, P., Fischer, P., and Allenspach, P. (**1989**). "Neutron-diffraction study of ErBa₂Cu₃O$_x$ in the composition range $6.1 \leqslant x \leqslant 7.0$", Phys. Rev. B **40**, 4472–4476.

Samoylenkov, S. V., Gorbenko, O. Y, and Kaul, A. R. (**1997**). "An analysis of charge carriers distribution in RBa₂Cu₃O₇ using the calculation of bond valence sums", Phys. C **278**, 49–54.

Tallon, J. L. (**1990**). "The relationship between bond-valence sums and Tc in cuprate superconductors", Phys. C **168**, 85–90.

Tallon, J. L. (**1991**). "Time-dependent charge transfer and the superconducting phase diagram for YBa₂Cu₃O$_{7-\delta}$", Phys. C **176**, 547–550.

Williams, G. V. M. and Tallon, J. L. (**1996**). "Ion size effects on 7 and interplanar coupling in RBa₂Cu₃O$_{7-\delta}$", Phys. C **258**, 41–46.

Xiao, G., Cieplak, M. Z., Musser, D., Gavrin, A., Streitz, F. H., Chien, C. L., Rhyne, J. J., and Gotaas, J. A. (**1988**). "Significance of plane versus chain sites in high-temperature oxide superconductors", Nature **332**, 238–240.

Xu, Y., Ata-Allah, S. S., Berger, M. G., and Glück, O. (**1996**). "Rare-earth ion size effect on resistivity, susceptibility, and superconductivity of RBa₂ Cu$_{3-x}$Zn$_x$O$_{7-y}$ (r = Yb, Er, Y, Dy, Gd, Eu, Sm, and Nd)", Phys. Rev. B **53**, 15245–15253.

Yu, J., Jin, W. T., Zhao, Y., and Zhang, H. (**2009**). "Stable bonds and unstable bonds in Y(Pr)-123 system", Phys. C **469**, 967–969.

Zhang, H., Cheng, L. L., Qin, X. C., and Zhao, Y. (**2000**). "Combinative energy between two structural blocks and its correlation with superconductivity in Bi and Hg superconducting systems", Phys. Rev. B **61**, 1618–1622.